10

Learning Patterns in Images

Ryszard Michalski, Azriel Rosenfeld, Zoran Duric, Marcus Maloof, Qi Zhang

ABSTRACT

This chapter concerns problems of learning patterns in images and image sequences, and using them for interpreting new images. The chapter concentrates on three problem areas: (i) semantic interpretation of color images of outdoor scenes, (ii) detection of blasting caps in x-ray images of luggage, and (iii) recognizing actions in video image sequences. It discusses the image formation processes in these problem areas, and the choices of representation spaces used in our approaches to solving these problems. The results presented indicate the advantages of applying machine learning to vision.

10.1 INTRODUCTION

The underlying motivation of this research is that vision systems need learning capabilities for handling problems for which algorithmic solutions are unknown or difficult to obtain. Learning capabilities can also make vision systems more easily adaptable to different vision problems, and more flexible and robust in handling variable perceptual conditions [MRA94].

Much of the current research on learning in vision systems has concentrated on neural network applications — for example, road navigation [Pom91] and object detection and recognition in various types of images (visible, SAR, etc.) [FeB96, RBP96, RBK96]. Advantages of these methods include their generality and their ability to learn continuous transformations. Disadvantages include the difficulty of incorporating prior knowledge (especially relational knowledge), the difficulty of learning complex structural knowledge, slow learning rates, and lack of comprehensibility of the learned knowledge [MRA94].

While symbolic learning methods suffer much less from these problems, they have been applied mostly in areas other than computer vision. In computer vision, they may be particularly useful for new feature generation, learning visual surface descriptions like textures, learning complex shape descriptions, acquisition of structural or relational models of objects, construction and updating of model databases, scene segmentation, learning the "context" in which an algorithm can be successfully applied, and so forth [GrP96, MDMR96, MRADMZ96, StF95]. Applications of symbolic approaches to vision problems remain an insufficiently explored but potentially fruitful domain of research.

Multistrategy learning systems combine different representations and/or different learning algorithms. One particular multistrategy system combines neural network and symbolic learning. This method induces rules which are used to structure a neural network architecture. A secondary learning step refines the network's weights. This method provides generality and very fast recognition rates [BMP94, MZMB96]. One can also use neural networks for lower-level vision processes and symbolic methods for higher-level visual processes. These methods are potentially very powerful and promising directions of research.

We have been studying the application of symbolic, neural net and multistrategy learning methods to such problems as interpreting outdoor scenes, recognizing objects in cluttered environments, and recognizing actions in video image sequences. The following sections summarize specific results obtained on a project on "Computer vision through learning" being conducted jointly by George Mason University and the University of Maryland [MRADMZ96].

In Section 10.2 we review previous work on machine learning in computer vision. In Section 10.3 we address the problem of conceptually segmenting color images of outdoor scenes. For this purpose we use the Multi-level Image Sampling and Transformation (MIST) methodology; a detailed description of this methodology can be found in [MZMB96]. In Section 10.4 we address the problem of detecting blasting caps in x-ray images of luggage; the details can be found in [MaM96, MDMR96]. Finally, in Section 10.5 we address the problem of recognizing a function of an object from its motion; the technical details can be found in [DFR96, DRR96].

10.2 PREVIOUS WORK ON MACHINE LEARNING IN COMPUTER VISION

Michalski [Mic72, Mic73] examined how symbolic AQ rule learning could be used for discrimination between textures or between simple structures. These seminal papers presented the Multi-Level Logical Template (MLT) methodology in which windowing operators scanned an image and extracted local features. These features were used to learn rules describing textures (or simple structures); the rules were then used for texture (or simple structure) recognition.

Shepherd [She83], encoding examples as feature vectors, learned decision trees for an industrial inspection task — specifically, classification of the shapes of chocolates. Comparisons of classification accuracy were made between decision tree, k-nearest neighbor (k-nn), and minimum distance classifiers. Experimental results for these classifiers were similar, with the minimum distance classifier producing the highest accuracy, 82%.

Channic [Cha89] extended the MLT methodology [Mic72, Mic73] by using convolution operators in conjunction with the original set of windowing operators for feature extraction. Using the AQ learning system, Channic investigated incremental learning and iterative learning from sequences of images using ultrasound images of laminated objects.

Instead of representing examples using feature vectors, Connell and Brady [CoB87] learned generalized semantic networks from images of classes of hammers and of overhead views of commercial aircraft. Training examples were generated by a vision system that took gray scale images as input and produced semantic networks for the objects. A learning system, which was a modified version of Winston's [Win84] ANALOGY program, learned by generalizing the training examples. The learning system was extended to learn disjunctive concepts and to learn from only positive examples. These generalized representations were used to classify unknown objects.

Cromwell and Kak [CrK91] proceeded as Shepherd did, using feature vectors to characterize shapes. Electrical component shapes were learned using a symbolic induction methodology based on that developed by Michalski [Mic80]. They reported that their method achieved 72% on testing data, but no comparisons were made to other learning methods.

Pachowicz and Bala [PaB91] also used the MLT methodology, following Michalski [Mic72, Mic73] and Channic [Cha89], but added a modified set of Laws' masks for texture feature extraction. They also applied techniques for handling noise in symbolic data. These techniques included optimizing learned symbolic descriptions by truncating rules [MMHL86], as well as removing training examples covered by weak rules and re-learning. The PRAX method for learning a large number of classes was introduced by Bala, Michalski, and Wnek [BMW92, BMW93].

Segen [Seg94] used a hybrid shape representation consisting of a hierarchical graph that takes into account local features of high curvature, and the angles and distances between these local features. This representation is invariant to both planar rotation and translation. Shapes were silhouettes of hand gestures. Segen's system runs in real time and has been applied to airplane simulator control as well as to control of a graphics editor program. Error rates were between 5% and 10%, but most errors were unknowns rather than misclassifications.

Cho and Dunn [ChD94] described a new learning algorithm for learning shape. This algorithm memorizes property lists and updates associated weights as training proceeds. Forgetting mechanisms remove useless property lists. Shapes are modeled by a series of line segments. Using the orientations of these segments, local spatial measures are computed and form a property list for a shape. The system was used to classify tools and hand gestures and achieved predictive accuracies of 92% and 96% on these problems.

Dutta and Bhanu [DuB94] presented a 3D CAD-based recognition system in which genetic algorithms are used to optimize segmentation parameters. Qualitative experimental results were presented for indoor and outdoor motion sequences in which the system recognized images of wedges (traffic cones) and cans from gray scale and depth map images.

Sung and Poggio [SuP94] worked on automatic human face detection. An example-based learning approach was tested for locating unoccluded frontal views of human faces in complex scenes. The space of human faces was represented by a few "face" and "non-face" pattern prototypes. At each image location, a two-valued distance measure was computed between the local image pattern and each prototype. A trained classifier was used to determine whether a human face is present. The authors showed that their distance metric is critical for the success of their system.

Zheng and Bhanu [ZhB96] examined how Hebbian learning mechanisms could be used to improve the performance of an image thresholding algorithm for automatic target detection and recognition. Qualitative results were presented in which the adaptive thresholding algorithm was shown to be superior to the classical thresholding algorithm for both SAR and FLIR images.

Rowley et al. [RBK96] built a neural network-based face detection system by using a retinally connected neural network to examine small windows of an image and decide on the existence of a face. A bootstrap algorithm was implemented during training so as to add false detection into the training set and as a consequence, eliminate the difficult task of manually selecting non-face training examples. Experimental results showed better performance in terms of detection and false-positive rates.

Romano et al. [RBP96] built a real-time system for face verification. Experiments showed that simple correlation strategies on template-based models are sufficient for many applications in which the identity of a face in a novel image must be verified quickly and reliably from a single reference image. The authors suggested that this automatic real-time face verification technique could be put to use in such human-machine interface applications as automated security systems. The technique has been integrated into a screen locking application which permits access to workstations by performing face verification in lieu of password authentication.

The MLT methodology [Mic72, Mic73] has recently been extended into the Multi-Level Image Sampling and Transformation (MIST) methodology. MIST has been applied to a variety of problems including natural scene segmentation [MZMB96] and identification of blasting caps in x-ray images [MDMR96]. For classifying natural scenes, three learning techniques were compared: AQ15c [WKBM95], a backpropagation neural network [Zur92], and AQ-NN [BMP94].

AQ-NN is a multistrategy learning technique in that it uses two different representations and two different learning strategies. Specifically, the AQ learning algorithm is used to learn attributional decision rules from training examples. These decision rules are then used to structure a neural network architecture. A backpropagation algorithm is then used as a learning step to further optimize the AQ induced descriptions. In such a system, learning times and recognition rates are often significantly decreased, while predictive accuracy is improved, with respect to conventional neural network learning. To learn classes such as ground, grass, trees and sky, hue, intensity, and convolution operators are used to extract features from a user-designated training area. These examples are then presented to the learning system, which induces a class description. AQ15c, used alone, achieved a predictive accuracy of 94%, while AQ-NN and a standard neural network achieved predictive accuracies near 100%. The training time of AQ-NN was approximately two orders of magnitude shorter than the training time of the standard NN.

10.3 SEMANTIC INTERPRETATION OF COLOR IMAGES OF OUTDOOR SCENES

The MIST methodology (Multi-level Image Sampling and Transformation) provides an environment for applying diverse machine learning methods to problems of computer vision. The methodology is illustrated here in connection with a problem of learning how to semantically interpret natural scenes. In the experiments described here, three learning programs were used: AQ15c for learning decision rules from examples; NN, neural network learning; and AQ-NN, multistrategy learning combining symbolic and neural network methods.

The results presented below illustrate the performance of the learning programs for the chosen problem of natural scene interpretation in terms of predictive accuracy, training time, recognition time, and complexity of the induced descriptions. The MIST methodology has proven to be very useful for this application. Overall, the experiments indicate that the multistrategy learning program AQ-NN appears to be the most promising approach.

This section briefly describes the MIST methodology and illustrates it by an application to natural scene interpretation. As pointed out in [FiS88, StF91], the semantic interpretion of natural scenes and recognition of natural objects is one of the most challenging open vision problems. The MIST methodology offers a new approach to these problems.

10.3.1 The MIST Methodology

The MIST methodology works in two basic modes: *Learning mode* and *Interpretation mode*. In Learning mode, the system builds or updates the Image Knowledge Base (IKB), which contains class descriptions and the background knowledge relevant to image interpretation. A description (or model) of a visual category is developed by inductive inference from examples specified by a trainer. Class descriptions are arranged into procedures defining sequences of image transformation operators.

In Interpretation mode, a learned (or predefined) image transformation procedure is applied to a given image to produce an Annotated Symbolic Image (ASI). In an ASI, areas that correspond to the locations of recognized classes in the original image are marked by symbols (e.g., colors) denoting these classes, and linked to annotations (text containing additional information about the classes, such as degree of certainty

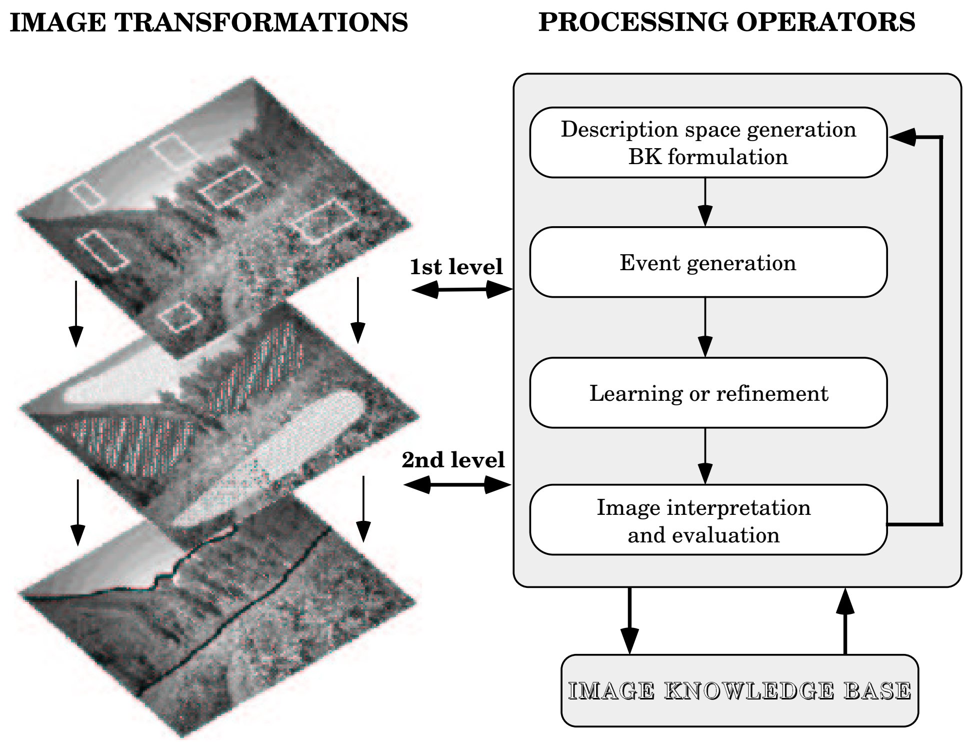

Figure 10.1 The MIST learning mode.

of recognition, properties of the class, relations to other classes, etc.). (Although developed independently, MIST's concept of an ASI is similar to the concept of a class map in the ALISA system [HoB94].) The following paragraphs describe the two modes in greater detail.

10.3.1.1 TRAINING MODE

This mode (see Figure 10.1) is executed in four phases: **LP1**—description space generation and background knowledge formulation; **LP2**—event generation; **LP3**—learning or refinement; and **LP4**—image interpretation and evaluation. These four phases can be repeated iteratively, creating images at different levels.

LP1: *Description space generation and background knowledge formulation*

A trainer assigns class names to areas in the image(s) that contain objects to be learned. These areas are divided into training and testing areas. Objects to be learned are presented in different poses and with different appearances (by changing perceptual conditions) so the system can learn a description that is invariant to class-preserving transformations. The trainer also defines the initial description space, i.e., initial attributes and/or terms to be measured on image samples, and specifies their value sets (measurement scale) and their types. This phase also involves an optimization of the image volume, that is, a reduction of the image resolution and intensity levels (hue and saturation, in color images) according to the needs of the given problem. The trainer may also define constraints on the description space, initial recognition rules, and possibly forms for expressing the descriptions (e.g., conjunctive rules, DNF, the structure of the neural network, etc.). Procedures for the measurement of attributes/terms are selected from a predefined collection.

LP2: *Event generation*

Using the chosen procedures, the system generates initial training examples ("training events") from each area. The areas are sampled exhaustively or selectively.

LP3: *Learning or refinement*

The system applies a selected machine learning program to the training examples to generate a class description. Currently, we have the following programs available: AQ15c for learning general symbolic rules from examples; NN, neural network learning with backpropagation; and AQ-NN, a system that integrates AQ rule learning with neural network learning.

LP4: *Image interpretation and evaluation*

The developed descriptions are applied to the testing areas to generate an *Annotated Symbolic Image* (ASI). In an ASI, the areas corresponding to given classes are marked by symbols representing these classes (numbers, colors, etc.). These areas are also linked to text that includes additional information about the class descriptions. The quality of the generated descriptions is determined by comparing the ASI with testing areas in the original image. Depending on the results, the system may stop, or may execute a new learning process (iteration), in which the ASI is the input (hence the term "multilevel" in the name of the methodology). If the generated descriptions need no further improvement, the process is terminated. This occurs when the obtained symbolic image is "sufficiently close" to the target image labeling (indicating the "correct" labeling of the image). Complete object descriptions are sequences of image transformations (defined by descriptions obtained at each iteration) that produce the final ASI. Learning errors are computed by comparing the target labeling (made by the trainer) with the learned labeling (produced by the system).

10.3.1.2 INTERPRETATION MODE

In this mode, the system applies descriptions from the Image Knowledge Base to semantically interpret a new image. To do so, the system executes a sequence of operators (defined by the description) that transform the given image into an ASI. A given "pixel" in the ASI is assigned a class on the basis of applying operators to a single event, or to a sample of events, and applying majority voting (typically within a 3×3 window). In ASI, different classes are denoted by different colors and/or textures. The simplest form of annotation used in the ASI is to associate degrees of confidence with the ASI pixels denoting a given class.

Figure 10.2 A typical image of a natural scene used in experiments.

10.3.2 Implementation and Experimental Results

The current MIST methodology has been implemented with the following learning systems:

- Symbolic rule learning program AQ15c [MMHL86, WKBM95].
- Multistrategy learning system AQ-NN combining decision rule learning with neural network learning [BMP94].
- Multistrategy learning system AQ-GA that combines decision rule learning with a genetic algorithm [MBP93].
- Class similarity-based learning for building descriptions of large numbers of classes (PRAX) [BMW92, BMW93].

An earlier version of MIST has been applied to learning descriptions of classes of surfaces [MBP93]. The core part of the descriptions was in the form of decision rules, which were determined by the inductive learning program AQ15 [MMHL86] and represented in the VL_1 logic-style language (Variable-Valued Logic System 1) [Mic73]. Such decision rules can be applied to an image in parallel or sequentially.

A simple version of the MIST methodology was applied to problems of semantically interpreting outdoor scenes using several learning methods. In the experiments, we used a collection of images representing selected mountain scenes around Aspen, Colorado (see Figure 10.2).

The input to the learning process was a training image in which selected examples of the visual classes to be learned had been labeled by a trainer — for example, trees,

Table 10.1 A summary of results from learning to interpret the image in Figure 10.3a. Data computed for 161 training events and 150 testing events selected from the 10 × 10 training area.

Learning method	Training time	Recognition time	Accuracy
AQ15c	0.43s	1.000s	94.00%
AQ-NN	10.93s	0.016s	99.98%
NN	4.38s	0.033s	99.97%

sky, ground, road, and grass. We experimented with different sets of attributes defining the description space, images obtained under different perceptual conditions, different sizes of training areas, and different sources of training and testing image samples (from different parts of the same image area, from different areas of the same image, from different images).

In the experiments described here, the description space was defined by such attributes as hue, saturation, intensity, horizontal and vertical gradients, high frequency spots, horizontal and vertical V-shapes, and Laplacian operators. These attributes were computed for the 5×5 windowing operator (sample size) that scanned the training area. Vectors of attribute values constituted training events. Three learning methods were used: AQ15c, AQ-NN, and NN. Three different sizes of training areas were used: 10×10, 20×20, and 40×40 pixels. The validation methodology used here was a hold-out method in which a random selection of 60% of the samples from the training area were used for training, while the remaining 40% were used for testing [WeK92].

Table 10.1 gives results from an experiment involving only one level of image transformation using different learning programs. In this experiment, the training area for each class was only 10×10 pixels. When the training area was enlarged to 20×20, the training time was significantly longer, but the correctness of the interpretation of the areas of the image was approximately the same.

Figure 10.3 presents an example of a training image and an ASI obtained by applying the learned one-level descriptions to the whole image using a majority voting evaluation scheme. As can be seen from Figure 10.3b, most of the areas in the image were correctly interpreted, although the system learned class descriptions from relatively small training areas (Figure 10.3a). In this experiment, AQ-NN produced a slightly smaller neural network and the interpretation time was about 50% shorter than with the NN method.

We also tested the data-driven constructive induction method (AQ17-DCI) in this experiment; this resulted in some new attributes, but it gave comparable results [BWMK93].

10.4 DETECTION OF BLASTING CAPS IN X-RAY IMAGES OF LUGGAGE

This section presents work on an approach to the problem of recognizing blasting caps in x-ray images. This problem is an instance of a class of problems in which a vision

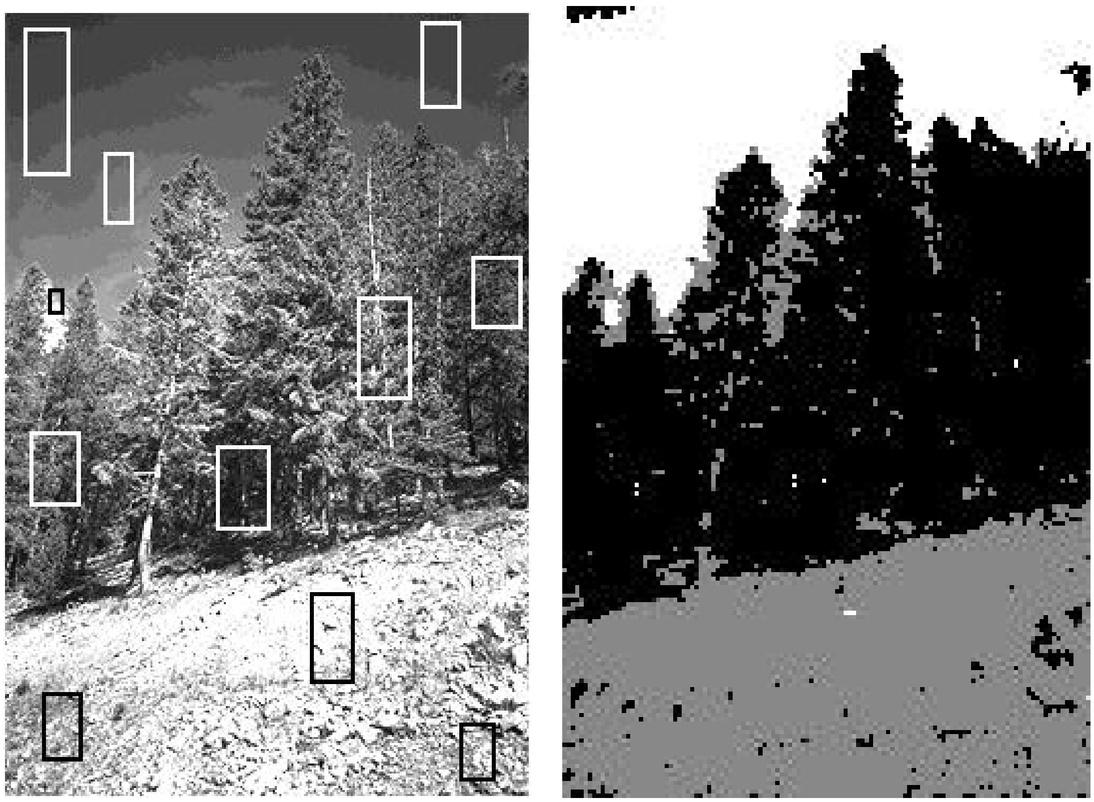

(a) (b)

Figure 10.3 An example of the image interpretation process based on the rules learned from the indicated training areas. (a) An image with training areas for for sky, tree, and ground. (b) ASI obtained using a majority voting scheme.

system must inspect a sequence of images for known objects. Unfortunately, the fact that the objects are known is often of little or no help. If there is little standardization of the class of known objects, it becomes impractical to attempt to model the objects geometrically. What often constrains a class of objects is functionality [FrN71, StB91a, RDR95]. Learning can be useful for acquiring the relationship between image characteristics and object functionality [WCHBS95].

Our primary focus is on investigating how vision and learning can be combined to find blasting caps, as well as objects that could occlude blasting caps, in x-ray images. In a previous study [MaM94, MaM96], learning was used to acquire descriptions of blasting caps. Simple segmentation techniques were used to isolate objects from their background; they were then represented using intensity and geometric features.

In the work presented here, an analysis of functional properties of blasting caps was

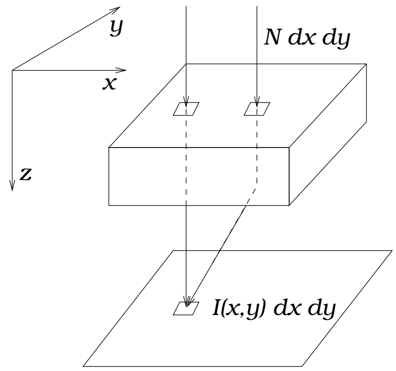

Figure 10.4 The geometry of x-ray imaging [Dan88].

conducted to design the representation space for learning, which combines intensity and shape features. Experimental results demonstrate the ability of the inductive learning system to acquire the relationship between image characteristics and object functionality.

This research provides an opportunity to study the interplay between vision and learning processes [MRA94], especially as it relates to learning object functionality. A vision system capable of reliably recognizing blasting caps or objects that could occlude blasting caps could be used to aid airport security personnel in luggage screening.

10.4.1 Preliminaries

In this section we review the image formation process and imaging model in x-ray images.

A typical x-ray imaging system consists of an x-ray tube (photon source), an anti-scatter device, and a receptor (photon detector) [Dan88]. The photons emitted by the x-ray tube enter the objects, where they may be scattered, absorbed or transmitted without interaction. The primary photons recorded by the image receptor form the image, but the scattered photons create a background signal (i.e., noise) that degrades contrast. In most cases, the majority of the scattered photons can be removed by placing an anti-scatter device between the objects and the image receptor.

What follows is a simple mathematical model of the imaging process. We start by considering a monochromatic x-ray source that emits photons of energy E and is sufficiently far from the objects (luggage) being inspected that the photon beam can be considered to be parallel (see Figure 10.4). The incident photon beam is parallel to the z direction and the image is recorded in the xy plane. We assume that each photon interacting with the receptor is locally absorbed and that the response of the receptor is linear, so that the image may be considered as a distribution of absorbed energy. If N photons per unit area are incident on the object and $I(x,y)\,dx\,dy$ is the energy absorbed in area $dx\,dy$ of the detector, then

$$I(x,y) = \exp\left(-\int \mu(x,y,z)dz\right) \cdot N\,\varepsilon(E,0)\,E\,(1+R)$$

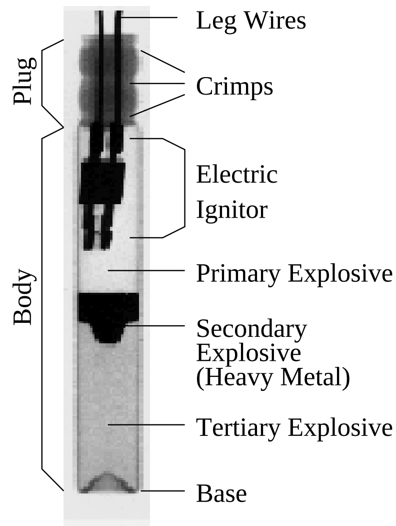

Figure 10.5 Detailed x-ray of a blasting cap.

where the line integral is over all materials along the path of the primary photons reaching the point (x, y), $\mu(x, y, z)$ is the linear attenuation coefficient, $\varepsilon(E, 0)$ is the energy absorption efficiency of the receptor for the photon energy level E at an incident angle of 0, and R is the ratio between the scattered and primary radiation (which is usually very small).

We assume orthographic image projection (see Figure 10.4). The image of the object point (X, Y, Z) is the point (x, y) such that

$$x = s\,X, \quad y = s\,Y,$$

where s is a constant. The image intensity at the pixel (x, y) is obtained by integrating $I(x, y)$ over the area of the pixel in the image receptor.

The intensity in an x-ray image is proportional to the number of x-ray photons that pass through objects on their way from the source to the receptor. Since different materials have different transparency properties, the intensity of an x-ray image depends on both the thickness and the type of material between the source and the receptor. Moreover, any x-ray photon that is not absorbed by one object on its path may be absorbed by another. Thus, a thick layer of semi-transparent material can have the same effect on the image receptor as a thin layer of opaque material.

10.4.2 Problem Statement

Although blasting caps are manufactured objects, there is enough variability in their manufacture to make a CAD-based recognition system impractical. What is common to all blasting caps, however, is their functionality. Ultimately, blasting caps are defined by their functional properties, not by their shapes.

A typical blasting cap (see Figure 10.5) consists of a cylindrical metal shell filled primarily with the explosive. In its approximate middle, there is a small globule of heavy metal secondary explosive. Finally, leg wires from the electric ignitor extend from one of the ends. The most dense (opaque to x-rays) part of a blasting cap is the concentration of the heavy metal explosive, which is approximately centrally symmetric. The leg wires also produce dense features, but are very thin. Finally, the copper or aluminum tube filled with explosive, which is axially symmetric, is typically more dense than the surrounding areas of the luggage.

To understand images of blasting caps, we begin by considering a generic blasting cap that is not occluded by opaque material. Let l be the length of an approximately cylindrical blasting cap, r be its radius, and σ be the angle between the axis of the cap and the image receptor. Consider the length of the path p of an x-ray photon as it passes through the blasting cap. When $\sigma = 0$, p ranges from $2r$ at the axis to 0 at the occluding contour. In general, p is multiplied by $\sec\sigma$; however, p cannot be longer than l. From the equation of $I(x, y)$, we see that the number of photons passing through the blasting cap decreases exponentially as p grows. From the image projection equations, we see that the image of a blasting cap is rectangularly shaped; its width is approximately $2rs$, and its length is approximately $ls\sec\sigma$. Its intensity is lowest along its axis, and highest along its occluding contour, which produces a low-contrast boundary. Also, the image of the heavy metal secondary explosive (see Figure 10.5) appears as a small, approximately symmetric blob on the axis of the blasting cap. The center of the blob is nearly opaque and thus its intensity is near zero. The boundary of the blob is lighter, but still has a very low intensity. The leg wires are strong features, but are not clearly visible in the images. (In our examples, the image resolution is 565×340 and the leg wires are barely visible. Currently, we are attempting to obtain images of higher resolution so that the leg wires can be more easily detected.)

Therefore, the strongest feature of a blasting cap is the low-intensity blob in the center of a rectangular ribbon of higher intensity. The intensities of both the blob and the ribbon are lowest along the axis of the blasting cap and highest along the occluding contour. Finally, if a blasting cap is occluded by any object, its image will be darker than the image of a blasting cap that is not occluded.

10.4.3 The Method and Experimental Results

We present a two-phase, bottom-up and top-down learning approach to recognizing blasting caps in x-ray images. In the first phase, low intensity blobs, which serve as attention-catching devices, are used to generate object hypotheses. These blobs correspond to the secondary high explosive, which is typically a heavy metal compound, located near the middle of the blasting cap (see Figure 10.5).

In the second phase, each generated hypothesis spawns a process that attempts to fit a local model to ribbon-like features surrounding the blob. These features correspond to the metal body of the blasting cap (see Figure 10.5). The local model is acquired using the inductive learning system AQ15c and captures intensity and geometric features of both the low intensity blob and the surrounding ribbons. A flexible matching

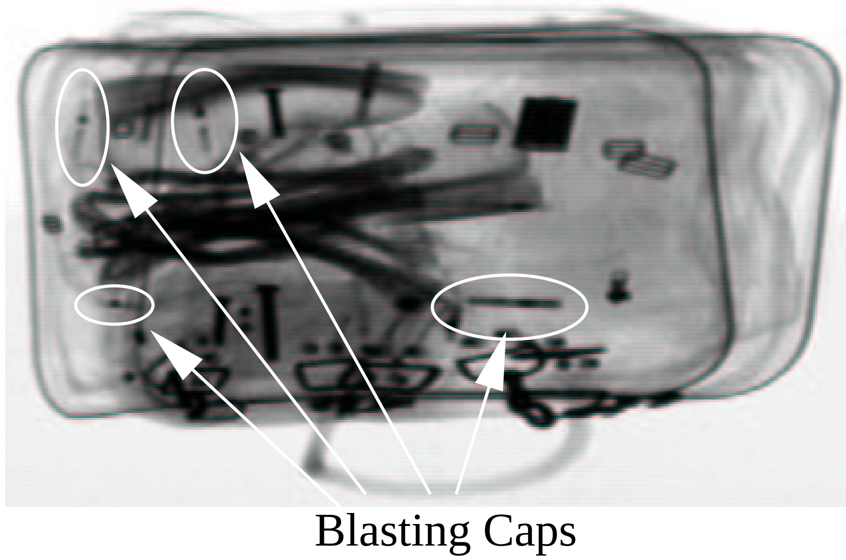

Figure 10.6 Sample image used for experimentation.

routine is used to match the local model to the image characteristics; this not only produces an object identification, but also yields a confidence in the identification.

The x-ray images used for experimentation were of luggage containing blasting caps appearing in varying orientations and under varying amounts of clutter, which included clothes, shoes, calculators, pens, batteries, and the like. The luggage was imaged much as it would be in an airport scenario: flat in relation to the x-ray source, but rotated in the image plane. Five images were selected from a set of 30 which were of low to moderate complexity in terms of clutter and positional variability of the blasting cap. Figure 10.6 shows one of the images used for experimentation.

Regions of interest were interactively determined, and contained low intensity blobs and ribbons corresponding to positive and negative examples of blasting caps. From each of the 64 selected regions, 27 geometric (e.g., compactness and proximity measures) and intensity-based (e.g., minimum, maximum, and average) features were computed, resulting in 28 blasting cap and 38 non-blasting cap objects. The AQ15c [WKBM95] inductive learning system was used to learn descriptions of blasting caps and non-blasting caps.

Induced descriptions from AQ15c were validated using 100 iterations of two-fold cross-validation. This validation method involves 100 learning and recognition runs. For each run, the extracted image data was randomly partitioned into a training set and a testing set. After learning from examples in the training set, the induced class definitions were tested using examples in the testing set. We can compute the predictive accuracy for each run based on the correct or incorrect classification of the examples in the testing set. The overall predictive accuracy for the experiment is the average of the accuracies computed for each run. These results are summarized in

Table 10.2 Summary of quantitative experimental results.

Average Predictive Accuracy (%)		
Overall	Correct	83.51±1.3
	Incorrect	16.49±1.3
Blasting Cap	Correct	85.82±2.1
	Incorrect	14.18±2.1
Non-Blasting Cap	Correct	81.19±2.4
	Incorrect	18.81±2.4

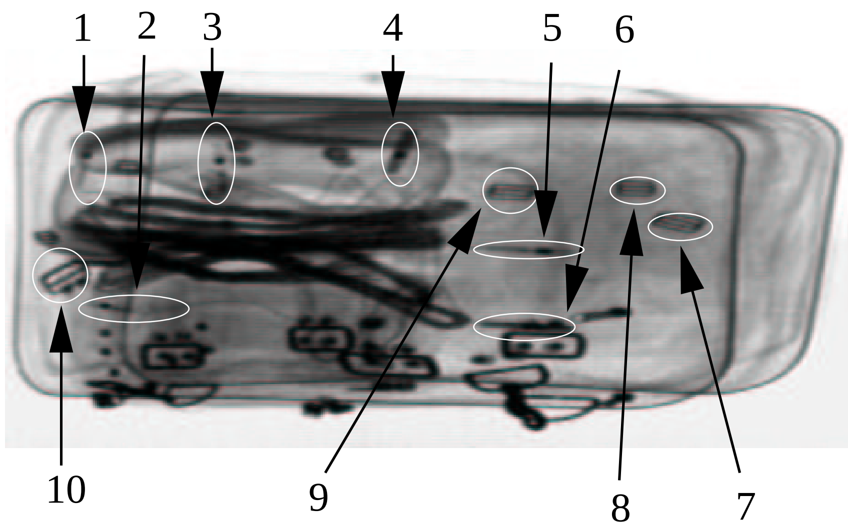

Figure 10.7 Test image for applying learned class definitions.

Table 10.2 and show the average predictive accuracy with a 95% confidence interval for the overall experiment and for each class.

As a qualitative demonstration of the method, the learned class definitions were also applied to an unseen image. The learned class definitions from AQ15c using training data from four images were tested on objects extracted from a fifth, unseen image, which is shown in Figure 10.7. Objects 1–6 are blasting caps, objects 7–10 are not. Object 5, which is a blasting cap, was mis-classified. All other objects in this image were classified correctly.

10.5 RECOGNIZING ACTIONS IN VIDEO IMAGE SEQUENCES

Recognizing the functions of objects is often a prerequisite to interacting with them. The functionality of an object can be defined as the usability of the object for a particular purpose [BoB94].

There has been considerable recent research on the problem of recognizing object functionality; for a short survey see [BoB94]. Early work on functional recognition can be found in [FrN71, SoB83, WBKL83]. The goal of this research has been to determine functional capabilities of an object based on characteristics such as shape, physics and causation. More recently, Stark and Bowyer [StB91a, StB91b, SHGB93] used this approach to solve some of the problems presented by more traditional model-based methods of object recognition. This work has dealt only with stationary objects; no motion is involved. In more recent work Green et al. [GESB94] discuss the recognition of articulated objects, using motion to determine whether the object possesses the appropriate functional properties. Little attention has been given to the problem of determining or learning the functionality of an object from its motion. In fact, however, motion provides a strong indication of function. In particular, velocity, acceleration, and force of impact resulting from motion strongly constrain possible function. As in other approaches to recognition of function, the object (and its motion) should not be evaluated in isolation, but in context. The context includes the nature of the agent making use of the object and the frame of reference used by the agent.

In this section, we address the following problem: How can we use the motion of an object, while it is being used to perform a task, to determine its function? Our method of answering this question is based on the extraction of a few motion descriptors from the image sequence. These descriptors are compared with stored descriptors that arise in known motion-to-function mappings to obtain function recognition.

Since many objects can display similar motion characteristics an object model is necessary to determine the functions of objects from their motion characteristics. Our work is based on segmenting the object into primitive parts and analyzing their motions.

10.5.1 Function from Motion

10.5.1.1 PRIMITIVE SHAPES AND PRIMITIVE MOTIONS

Following [Bie85, RRP93, RDR95] we regard objects as composed of primitive parts. On the coarsest level we consider four types of primitive parts: sticks, strips, plates, and blobs, which differ in the values of their relative dimensions. As in [RDR95] we let a_1, a_2, and a_3 represent the length, width, and height of a volumetric part. We can then define the four classes as follows:

$$\begin{aligned} Stick: &\quad a_1 \simeq a_2 \ll a_3 \vee a_1 \simeq a_3 \ll a_2 \vee a_2 \simeq a_3 \ll a_1 \\ Strip: &\quad a_1 \neq a_2 \wedge a_2 \neq a_3 \wedge a_1 \neq a_3 \\ Plate: &\quad a_1 \simeq a_2 \gg a_3 \vee a_1 \simeq a_3 \gg a_2 \vee a_2 \simeq a_3 \gg a_1 \end{aligned}$$

$$Blob: \qquad a_1 \simeq a_2 \simeq a_3$$

If all three dimensions are about the same, we have a blob. If two are about the same, and the third is very different, we have two cases: if the two are bigger than the one, we have a plate, and in the reverse case we have a stick. When no two dimensions are about the same we have a strip. For example, a knife blade is a strip, because no two of its dimensions are similar.

Primitives can be combined to create compound objects. In [RDR95] the different qualitative ways in which primitives can be combined were described—for example, end to end, end to side, end to edge, etc. In addition to specifying the two attachment surfaces participating in the junction of two primitives, we could also consider the angles at which they join, and classify the joints as perpendicular, oblique, tangential, etc. Another refinement would be to describe qualitatively the position of the joint on each surface; an attachment can be near the middle, near a side, near a corner, or near an end of the surface. We can also specialize the primitives by adding qualitative features such as axis shape (straight or curved), cross-section size (constant or tapered), etc.

Functional recognition is based on compatibility with some action requirement. Some basic "actions" are static in nature (supporting, containing, etc.), but many actions involve using an object while it is moving. To illustrate the ways in which a primitive shape can be used, consider the action of "cutting" with a sharp strip or plate. Here a sharp edge is interacting with a surface. The interaction can be described from a kinematic point of view. The direction of motion of the primitive relative to its axis defines the type of action—for example, stabbing, slicing or chopping. These actions all involve primitive motions, which we define to be motions (translations or rotations) along, or perpendicular to, the main axes of the primitive. In this section we will use the detection of primitive motions to infer an object's function.

10.5.1.2 INFERRING OBJECT FUNCTION FROM PRIMITIVE MOTIONS

Given a moving object as seen by an observer, we would like to infer the function being performed by the object. The object is given as a collection of primitives. For example, a knife can be described as consisting of two primitives: a handle (a stick) and a blade (a strip). Given this model, the system estimates the pose of the object (as in [RDR95]) and passes this information to the motion estimation module. The model and the results of the motion estimation enable the system to infer the function that is being performed by the object.

The function being performed by an object depends on the object's motion both in the object's coordinate system and relative to the object it acts on (the "actee"). This information gives us the relationships between the direction of motion, the main axis of the object, and the surface of the actee, and these relationships can be used to determine the intended function. For example, we would expect the motion of a knife that is being used to "stab" to be parallel to the main axis of the knife, whereas if the knife is being used to "chop" we would expect motion perpendicular to the main axis.

In both cases, the motion is perpendicular to the surface of the actee. If the knife is being used to slice, we would expect back-and-forth motion parallel to its main axis and also parallel to the surface of the actee.

10.5.2 Computing Motion

10.5.2.1 MOTIONS OF STICKS AND STRIPS

Consider a moving object $\mathcal{B}$. There is an *ellipsoid of inertia* associated with $\mathcal{B}$. The center of the ellipsoid is at the center of mass C of $\mathcal{B}$; the axes of the ellipsoid are called the *principal axes*. We associate the coordinate system $Cx_1y_1z_1$ with the ellipsoid and choose the axes of $Cx_1y_1z_1$ to be parallel to the principal axes. Let $\vec{\imath}_1$ be the unit vector in the direction of the longest axis l_c (this axis corresponds to the smallest principal moment of inertia); let $\vec{k}_1$ be the unit vector in the direction of the shortest principal axis (this axis corresponds to the largest moment of inertia); and let $\vec{\jmath}_1$ be the unit vector in the direction of the remaining principal axis with the direction chosen so that the vectors $(\vec{\imath}_1, \vec{\jmath}_1, \vec{k}_1)$ form a right-handed coordinate system.

Here we consider only objects that are approximately planar, straight strips and sticks. For a planar strip the axis of the maximal moment of inertia is orthogonal to the plane of the strip; if the strip is approximately straight, the axis of the minimal moment of inertia is approximately parallel to the medial axis l_c of the strip. In the case of a straight stick, similarly, l_c corresponds to the longest principal axis of the ellipsoid of inertia; the other two principal axes are orthogonal to l_c and can be chosen arbitrarily. We assume that the motion of the stick or strip is planar and that the plane is "visible" to the observer. (The "visibility" constraint allows an oblique view as long as the angle between the surface normal and the z-axis of the camera is $\leq 30°$ (say).) When the object is a strip we assume that the motion is in the plane of the strip; the translational velocity is then parallel to the plane of the strip and the rotational velocity is orthogonal to the plane of the strip. When the object is a stick the consecutive positions of the stick define the motion plane; the translational velocity lies in the plane and the rotational velocity is orthogonal to the plane. In this case we choose the axis of minimal moment of inertia to be orthogonal to the plane of the motion.

10.5.2.2 COMPUTING PRIMITIVE MOTIONS

We now briefly review our method of computing primitive motions of sticks and strips. A complete description of the method can be found in [DRR96, DFR96].

We associate two rectangular coordinate frames with a rigidly moving body $\mathcal{B}$, one $(Oxyz)$ fixed in space (the camera frame), the other $(Cx_1y_1z_1)$ fixed in the body $\mathcal{B}$ and moving with it (the object frame). The position of the moving frame at any instant is given by the position $\vec{d}_c = (X_c \;\; Y_c \;\; Z_c)^T$ of the origin C (the center of mass of $\mathcal{B}$), and by the nine direction cosines of the axes of the moving frame with respect to the fixed frame. The pair $(\vec{\omega}, \vec{T})$, where $\vec{\omega} = (A \;\; B \;\; C)^T$ is the rotational velocity of the moving frame and $\dot{\vec{d}}_c = (\dot{X}_c \;\; \dot{Y}_c \;\; \dot{Z}_c)^T \equiv (U \;\; V \;\; W)^T \equiv \vec{T}$ is the translational velocity of the point C, defines the motion of $\mathcal{B}$. The rotational velocity in the moving frame is $\vec{\omega}_1 = (A_1 \ \ B_1 \ \ C_1)^T$; we can write $\vec{\omega} = R\vec{\omega}_1$ and $\vec{\omega}_1 = R^T\vec{\omega}$, where R is the matrix of the direction cosines. From our assumptions about the motion of $\mathcal{B}$ we have $\vec{\omega}_1 = C_1\vec{k}_1$ and $\vec{T}_1 = U_1\vec{\imath}_1 + V_1\vec{\jmath}_1$.

Let f be the focal length of the camera and let Z_c be the depth of the center of mass C of $\mathcal{B}$. The weak perspective projection of the scene point (X, Y, Z) onto the image point (x, y) is given by

$$x = \frac{X}{Z_c}f, \quad y = \frac{Y}{Z_c}f.$$

For the instantaneous velocity of the image point (x, y) under weak perspective projection we have [DFR96]

$$\begin{aligned} \dot{x} &= \frac{Uf - xW}{Z_c} - C_1(y - y_c)N_z - C_1[(x - x_c)N_xN_y/N_z + (y - y_c)N_y^2/N_z], \\ \dot{y} &= \frac{Vf - yW}{Z_c} + C_1(x - x_c)N_z + C_1[(x - x_c)N_x^2/N_z + (y - y_c)N_xN_y/N_z], \end{aligned}$$

where (x_c, y_c) is the image of (X_c, Y_c) and $\vec{N} = (N_x \ N_y \ N_z)^T = R\vec{k}_1$ is the normal to the plane of motion; we have also used the fact that $\vec{\omega} = R\vec{\omega}_1$.

If we choose a unit direction vector $\vec{n}_r = n_x\vec{\imath} + n_y\vec{\jmath}$ (usually the direction of the image intensity gradient) at the image point (x, y) and call it the normal direction, then the *normal motion field* at (x, y) is $\dot{\vec{r}}_n = (\dot{\vec{r}} \cdot \vec{n}_r)\vec{n}_r$. We then have $\dot{\vec{r}}_n = (\dot{x}n_x + \dot{y}n_y)\vec{n}_r$.

Let $I(x, y, t)$ be the image intensity function. Given the image gradient ∇I and the partial derivative in time I_t of I we have

$$\vec{u}_n = \frac{-I_t \nabla I}{\|\nabla I\|^2}$$

where $\vec{u}_n$ is called the *normal flow.*

The magnitude of the difference between $\vec{u}_n$ and the normal motion field $\dot{\vec{r}}_n$ is inversely proportional to the magnitude of the image gradient. Hence $\dot{\vec{r}}_n \approx \vec{u}_n$ when $\|\nabla I\|$ is large. Expression for the normal flow thus provides an approximate relationship between the 3-D motion and the image derivatives. In [DFR96, DRR96] the normal flow (an observable quantity) was used as an approximation of the projected motion field. The method of least squares estimation was used to obtain the estimates of C_1, U/Z_c, V/Z_c, and W/Z_c. These estimates and the fact that the object was "visible" were then used to obtain the values of U_1/Z_c and V_1/Z_c.

10.5.2.3 PARAMETRIZING THE MOTION OF A STICK OR STRIP

We use three angles α, β, and θ to parametrize the motions of sticks and strips.

The direction α of the medial axis is found using the following algorithm:

1 - Make a sorted (circular) list of all edge elements (sorted by their orientations modulo π) for which the normal flow is computed.

2 - Find the shortest segment $[\gamma_1, \gamma_2]$ such that more than $3/4$ of the orientations in the list are contained within it.
3 - Find the median orientation α in the sorted sublist chosen in the previous step.
4 - If α does not approximately agree with the pose that was estimated earlier, then $\alpha \leftarrow \alpha + \pi$.
5 - Use α as the orientation of the medial axis.

We estimate (x_c, y_c) — the image position of C (the reference point and the center of mass of the object)—as the average of the coordinates of all edge points for which the normal flow is computed.

We define β as the angle between the vector $(U_1 \;\; V_1 \;\; 0)^T$ and the Cx_1 axis of the tool coordinate system; thus

$$\beta = \arctan \frac{V_1}{U_1}.$$

We define θ to be the total rotation angle as a function of time:

$$\theta = \int_0^t C_1 dt.$$

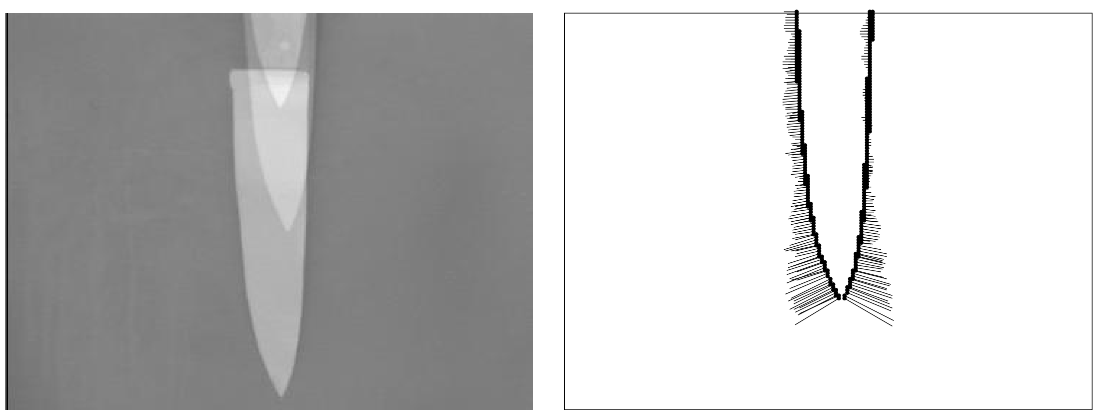

(a) (b)

Figure 10.8 (a) Stabbing motion. (b) Flow vectors for Stabbing.

10.5.3 Experiments

In our experiments we observed the motion of a knife performing a task. The vision system took images at 25 frames per second for 5 seconds, yielding 125 images per experiment. After each image sequence was recorded, a representative sampling of the 125 images was used for further processing. Eleven evenly spaced samples, each composed of three consecutive images, were used. (For instance, samples 1 and 2 in

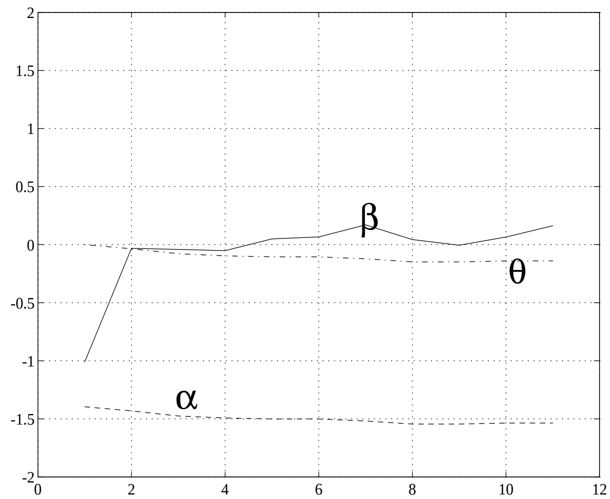

Figure 10.9 Angles α, β, and θ for Stabbing.

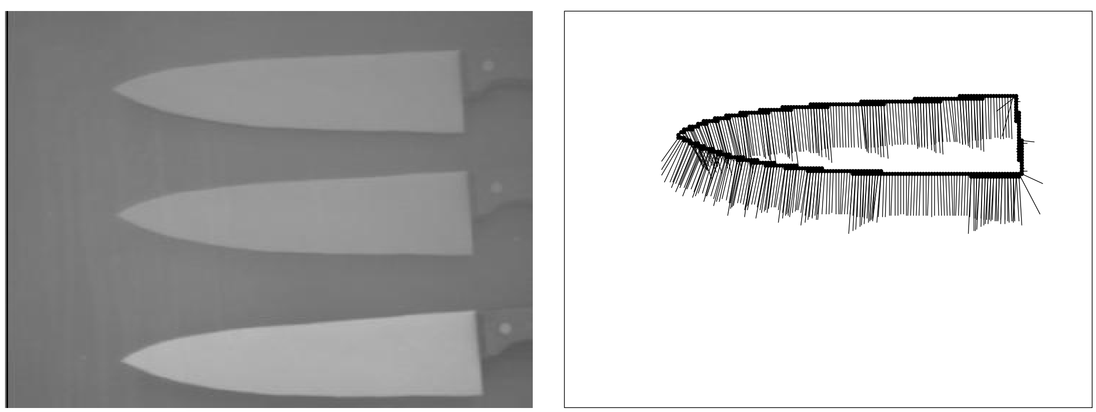

(a) (b)

Figure 10.10 (a) Chopping motion. (b) Flow vectors for Chopping.

any given experiment used images 0–2 and 10–12, respectively.) This resulted in 33 images for each experiment.

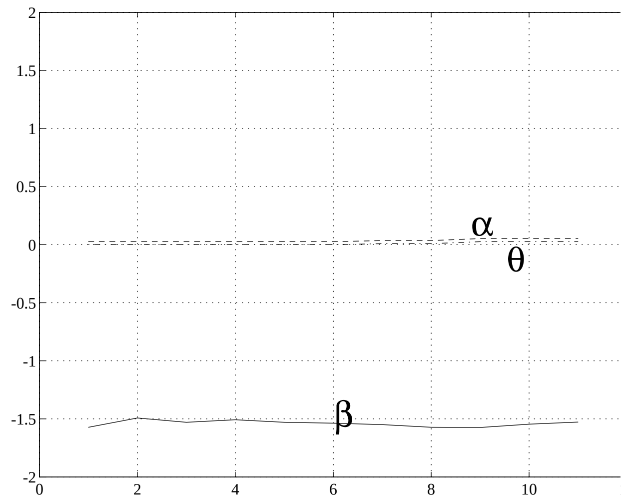

Figure 10.11 Angles α, β, and θ for Chopping.

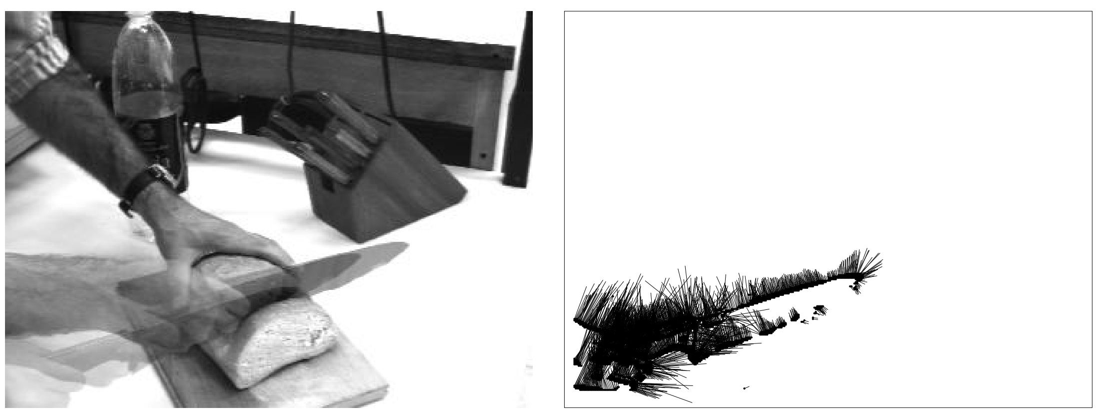

(a) (b)

Figure 10.12 (a) Slicing motion. (b) Flow vectors for Slicing.

10.5.3.1 STABBING

Stabbing is defined as the cutting motion of a knife in which α (the angle between the projection of l_c onto the plane $Z = Z_c$ and the Ox axis) is close to either $-\pi/2$ or $\pi/2$, β is approximately 0, and θ is small and approximately constant.

Figure 10.8 shows the flow vectors taken from the 6th sample and a composite image

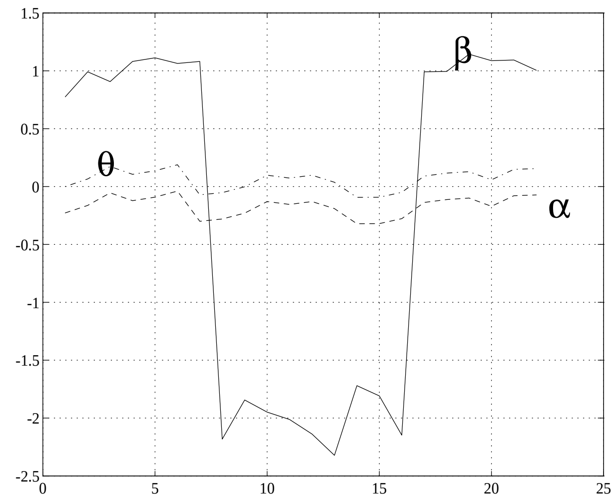

Figure 10.13 Angles α, β, and θ for Slicing.

of the knife taken from the 1st, 6th and 11th samples of the stabbing experiment. Figure 10.9 shows a plot of the triple (α, β, θ) with respect to time (frame numbers). We see that as was expected, the values of α are very close to $-\pi/2$, β is close to 0, and θ is close to 0. A VL_1 rule (Michalski [Mic72]) describing stabbing would be

$$< \textit{stabbing} > \; <:: \quad [\alpha = -1.55 \,..\, -1.35] \;\&\; [\beta = -1 \,..\, 0.2] \;\&\; [\theta = -0.2 \,..\, 0].$$

10.5.3.2 CHOPPING

Chopping is defined as the cutting motion of a knife in which α (the angle between the projection of l_c onto the plane $Z = Z_c$ and the Ox axis) is close to either 0 or π, β is close to $\pi/2$ (when $\alpha \approx \pi$) or $-\pi/2$ (when $\alpha \approx 0$), and θ is small and approximately constant.

Figure 10.10 shows the flow vectors taken from the 6th sample and a composite image of the knife taken from the 1st, 6th and 11th samples of the chopping experiment. Figure 10.11 shows a plot of the triple (α, β, θ) with respect to time (frame numbers). We see that, as was expected, the values of α are very close to 0, β is close to $-\pi/2$, and θ is close to 0. A VL_1 rule describing chopping would be

$$< \textit{chopping} > \; <:: \quad [\alpha = 0] \;\&\; [\beta = -1.6 \,..\, -1.5] \;\&\; [\theta = 0].$$

10.5.3.3 SLICING

Slicing is defined as the cutting motion of a knife in which α is approximately 0 (or $< \pi/2$), β oscillates between approximately 0 and approximately π, and θ is small and approximately constant.

Figure 10.12 shows the flow vectors taken from the 6th sample and a composite image of the knife taken from the 1st, 6th and 11th samples of the slicing experiment. (The mass of vectors at the left end of Figure 10.12a come from the motion of the hand, which is visible in the images.) Figure 10.13 shows a plot of the triple (α, β, θ) with respect to time (frame numbers). We see that, as was expected, the values of α are very close to 0, and that β oscillates between approximately $\pi/2$ and approximately $-3\pi/2$ (note that the two approximate values differ by π). A VL_1 rule describing slicing would be

$$\begin{aligned} < slicing > \quad <:: \quad & [\alpha = -0.25 \,..\, 0] \; \& \; [\beta = -2.25 \,..\, -1.75,\; 0.75 \,..\, 1.25] \; \& \\ & [\theta = -0.2 \,..\, 0] \; \& \; [T_\beta = 8..12] \end{aligned}$$

where T_β is the period of β (β changes between two ranges with the period T_β).

10.6 CONCLUSIONS AND FUTURE RESEARCH

10.6.1 Semantic Interpretation of Color Images of Outdoor Scenes

In Section 10.3 we showed that the MIST methodology can be very useful in applying machine learning methods to problems of natural scene interpretation. The results obtained so far have been promising, as they indicate a high level of performance accuracy even when only a single level of image transformation was applied. Particularly good results have been obtained with the AQ-NN method, which combines symbolic rule learning and a neural network.

There are several important advantages of this methodology. They include the ease of applying and testing diverse learning methods and approaches in a uniform manner, the potential for implementing advanced and complex learning processes, the use of background knowledge in learning and interpreting images, the suitability for parallel image learning and interpretation, and the ease of testing the performance of the methods.

Current research involves a systematic investigation of the methodology using different types of initial attributes and taking training and testing areas from images obtained under significantly different perceptual conditions.

10.6.2 Detection of Blasting Caps in X-ray Images of Luggage

In Section 10.4 we presented work in progress on the problem of recognizing blasting caps in x-ray images. In the first phase of a two-phase learning approach, low-intensity blobs were used as attention-catching devices. This bottom-up process was followed by a top-down recognition process in which a learned local model was matched to ribbon-shaped image regions surrounding a low-intensity blob. An analysis of the functional properties of blasting caps was used to design the representation space for learning, which combined intensity and geometric features. The experimental results suggest that learning can be used to acquire functional descriptions of objects. This is important for classes of objects for which geometric modeling is impractical.

Future work in this area will involve further automation of the feature extraction process and object labeling functions. In addition, other functional properties present in blasting caps still require exploitation. An example is the presence of leg wires (see Figure 10.5). Unfortunately, the current image set is not of a resolution that allows for the detection of these functional properties. We hope to acquire additional images that will be better suited for this type of analysis.

10.6.3 Recognizing Actions in Video Image Sequences

Perceiving function from motion provides an understanding of the way an object is being used by an agent. To accomplish this we combined information about the shape of the object, its motion, and its relation to the actee (the object it is acting on). Assuming a decomposition of the object into primitive parts, we analyzed a part's motion relative to its principal axes. Primitive motions (translation and rotation relative to the principal axes of the object) were dominating factors in the analysis. We used a frame of reference relative to the actee. Once such a frame is established, it can have major implications for the functionality of an action.

Several image sequences were used to demonstrate our approach. In the three sequences shown in Section 10.5, motion was used to discriminate between three cutting actions: stabbing, chopping, and slicing. In other sequences, not shown here [DFR96], we used motion information to differentiate between two different functionalities of the same object: scooping and hitting with a shovel, and hammering and tightening with a wrench.

Natural extensions of this work include the analysis of more complex objects. Complexity can be expressed in terms of either the shapes of the parts or the way in which the parts are connected. An interesting area is the analysis of articulated objects. The different types of connections between the parts constrain the possible relative motions of the parts. A pair of pliers or a pair of scissors is a simple case, with only a single articulated connection (one degree of freedom in the relative motion of the parts).

10.6.4 Advantages of Incorporating Learning into Vision Systems

We have given three illustrations of how a learning system can be used to help in handling vision problems for which algorithmic solutions are unknown or difficult to obtain. Specifically, we have studied the application of symbolic, neural network and multistrategy learning methods to the problems that involved interpreting outdoor scenes, recognizing objects in cluttered environments, and recognizing actions in video image sequences. The first problem involved segmentation of an image into regions corresponding to grass, trees, etc.; since these categories do not have simple definitions, optimal algorithms for discriminating them cannot easily be defined. The other two problems involved classes of objects or actions that do not have simple geometrical definitions, but are defined only functionally: detecting blasting caps in x-ray images of luggage, and recognizing types of cutting (stabbing, chopping, slicing) in video image sequences. In each of these cases we have been able to design an appropriate representation space to make learning (and recognition) feasible.

ACKNOWLEDGEMENTS

This research was supported in part by the Advanced Research Projects Agency under grants F49620-92-J-0549 and F49620-95-1-0462 administered by the Air Force Office of Scientific Research, in part by the Air Force Office of Scientific Research under grant F49620-93-1-0039, in part by the Advanced Research Projects Agency under grant No. N00014-91-J-1854 administered by the Office of Naval Research, in part by the Office of Naval Research under grant N00014-91-J-1351, and in part by the National Science Foundation under grants DMI-9496192 and IRI-9510644.

REFERENCES

[BMP94] Bala, J.W., Michalski, R.S., and Pachowicz, P.W., "Progress on vision through learning at George Mason University", in *Proc. ARPA Image Understanding Workshop*, 191–207, 1994.

[BMW92] Bala, J., Michalski, R.S., and Wnek, J., "The principal axes method for constructive induction", in *Proc. International Conference on Machine Learning*, D. Sleeman and P. Edwards (Eds.), Aberdeen, Scotland, 1992.

[BMW93] Bala, J., Michalski, R.S., and Wnek, J., "The PRAX approach to learning a large number of texture concepts", in *Proc. Machine Learning in Computer Vision: What, Why and How?, AAAI Fall Symposium on Machine Learning in Computer Vision*, 1993.

[Bie85] Biederman, I., "Human image understanding: Recent research and a theory", *Computer Vision, Graphics and Image Processing*, **32**:29–73, 1985.

[BWMK93] Bloedorn, E., Wnek, J., Michalski, R.S., and Kaufman, K., "AQ17 — A multistrategy learning system: The method and user's guide", *Reports of the Machine Learning and Inference Laboratory*, MLI 93-12, George Mason University, Fairfax, VA, 1993.

[BoB94] Bogoni, L. and Bajcsy, R., "Active investigation of functionality", in *Proc. CVPR Workshop on Visual Behaviors*, June 1994.

[BABC84] Brady, M., Agre, P.E., Braunegg, D.J., and Connell, J., II, "The mechanic's mate" in *Proc. European Conference on Artificial Intelligence*, 79–94, 1984.

[Cha89] Channic, T., "TEXPERT: An application of machine learning to texture recognition", *Reports of the Machine Learning and Inference Laboratory*, MLI 89-27, George Mason University, Fairfax, VA, 1989.

[ChD94] Cho, K. and Dunn, S.M., "Learning shape classes", *IEEE Transactions on Pattern Analysis and Machine Intelligence*, **16**:882–888, 1994.

[CrK91] Cromwell, R.L. and Kak, A.C., "Automatic generation of object class descriptions using symbolic learning techniques", in *Proc. National Conference on Artificial Intelligence*, 710–717, 1991.

[CoB87] Connell, J.H. and Brady, M., "Generating and generalizing models of visual objects", *Artificial Intelligence*, **34**:159–183, 1987.

[Dan88] Dance, D.R, "Diagnostic radiology with x-rays", in *The Physics of Medical Imaging*, S. Webb (Ed.), 20–73, IOP Publishing, Philadelphia, PA, 1988.

[DFR96] Duric, Z., Fayman, E., and Rivlin, E., "Function from motion", *IEEE Transactions on Pattern Analysis and Machine Intelligence*, 579–591, 1996.

[DRR96] Duric, Z., Rivlin, E., and Rosenfeld, A., "Learning an object's function by observing the object in action", in *Proc. ARPA Image Understanding Workshop*, 1437–1445, 1996.

[DuB94] Dutta, R. and Bhanu, B., "A learning system for consolidated recognition and motion analysis", in *Proc. ARPA Image Understanding Workshop*, 773–776, 1994.

[Fah88] Fahlman, S.E., "An empirical study of learning speed in back-propagation networks", Report CMU-CS-88-182, Carnegie-Mellon University, Pittsburgh, PA, 1988.

[FeB96] Ferryman, A. and Bhanu, B., "A Bayesian approach for the segmentation of SAR images using dynamically selected neigborhoods", in *Proc. ARPA Image Understanding Workshop*, 891–895, 1996.

[FiS88] Fischler, M.A. and Strat, T.M., "Recognizing trees, bushes, rocks and rivers", in *Proc. AAAI Spring Symposium Series: Physical and Biological Approaches to Computational Vision*, 62–64, 1988.

[FrN71] Freeman, P. and Newell, A., "A model for functional reasoning in design", in *Proc. International Joint Conference on Artificial Intelligence*, 621–640, 1971.

[GESB94] Green, K., Eggert, D., Stark, L., and Bowyer, K., "Generic recognition of articulated objects by reasoning about functionality", in *Proc. AAAI Workshop on Represening and Reasoning about Device Function*, 56–64, 1994.

[GrP96] Grimson, W.E.L. and Poggio, T., "Progress in image understanding at MIT", in *Proc. ARPA Image Understanding Workshop*, 65–74, 1996.

[HoB94] Howard, C.G. and Bock, P., "Using a hierarchical approach to avoid over-fitting in early vision", in *Proc. International Conference on Pattern Recognition*, 826–829, 1994.

[MDMR96] Maloof, M.A., Duric, Z., Michalski, R.S., and Rosenfeld, A., "Recognizing blasting caps in x-ray images", in *Proc. ARPA Image Understandning Workshop*, 1257–1261, 1996.

[MaM94] Maloof, M.A. and Michalski, R.S., "Learning descriptions of 2D blob-like shapes for object recognition in x-ray images: An initial study", *Reports of the Machine Learning and Inference Laboratory*, MLI 94-4, George Mason University, Fairfax, VA, 1994.

[MaM96] Maloof, M.A. and Michalski, R.S, "Learning descriptions of shape for object recognition in x-ray images", *Expert Systems with Applications*, in press, 1996.

[Mic72] Michalski, R.S., "A variable-valued logic system as applied to picture description and recognition", in F. Nake and A. Rosenfeld (Eds.), *Graphic Languages*, North-Holland, Amsterdam, 21–47, 1972.

[Mic73] Michalski, R.S., "AQVAL/1: Computer implementation of a variable-valued logic system VL_1 and examples of its application to pattern recognition", in *Proc. International Joint Conference on Pattern Recognition*, 3–17, 1973.

[Mic80] Michalski, R.S., "Pattern recognition as rule-guided inductive inference", *IEEE Transactions on Pattern Analysis and Machine Intelligence*, **2**:349–361, 1980.

[MBP93] Michalski, R.S., Bala, J.W, and Pachowicz, P.W., "Progress on vision through learning at George Mason University", in *Proc. ARPA Image Understanding Workshop*, 191–207, 1993.

[MMHL86] Michalski, R.S., Mozetic, I., Hong, J., and Lavrac, N., "The multipurpose incremental learning system AQ15 and its testing application to three medical domains", in *Proc. National Conference on Artificial Intelligence*, 1041–1045, 1986.

[MRA94] Michalski, R.S., Rosenfeld, A., and Aloimonos, Y., "Machine vision and learning: Research issues and directions — A report on the NSF/ARPA Workshop on Learning and Vision, Harpers Ferry, WV, October 15-17, 1992", *Reports of the Machine Learning and Inference Laboratory*, MLI 94-6, George Mason University, Fairfax, VA, 1994.

[MRADMZ96] Michalski, R.S., Rosenfeld, A., Aloimonos, Y., Duric, Z., Maloof, M.A., and Zhang, Q., "Progress on vision through learning: A collaborative effort of George Mason University and the University of Maryland", in *Proc. ARPA Image Understandning Workshop*, 177–187, 1996.

[MZMB96] Michalski, R.S., Zhang, Q., Maloof, M.A., and Bloedorn, E., "The multi-level image sampling and transformation methodology and its application to natural scene interpretation", in *Proc. ARPA Image Understandning Workshop*, 1473–1479, 1996.

[PaB91] Pachowicz, P.W. and Bala, J.W., "Texture recognition through machine learning and concept optimization", *Reports of the Machine Learning and Inference Laboratory*, MLI 95-4, George Mason University, Fairfax, VA, 1991.

[Pom91] Pomerleau, D.A., "Efficient training of artificial neural networks for autonomous navigation", *Neural Computation*, **3:**88–97, 1991.

[RDR95] Rivlin, E., Dickinson, S.J., and Rosenfeld, A., "Recognition by functional parts", *Computer Vision and Image Understanding*, **62:**164–176, 1995.

[RRP93] Rivlin, E., Rosenfeld, A., and Perlis, D., "Recognition of object functionality in goal-directed robotics", in *Proc. AAAI Workshop on Reasoning about Function*, 126–130, 1993.

[RBP96] Romano, R., Beymer, D., and Poggio, T., "Face verification for real-time applications", in *Proc. ARPA Image Understanding Workshop*, 747–756, 1996.

[RBK96] Rowley, H.A., Baluja, S., and Kanade, T., "Neural network-based face detection", in *Proc. ARPA Image Understanding Workshop*, 725–735, 1996.

[Seg94] Segen, J., "GEST: A learning computer vision system that recognizes hand gestures", in R.S. Michalski and G. Tecuci, (Eds.), *Machine Learning: A Multistrategy Approach*, Vol. IV, 621–634, Morgan Kaufmann, San Francisco, CA, 1994.

[She83] Shepherd, B.A., "An appraisal of a decision tree approach to image classification", in *Proc. International Joint Conference on Artificial Intelligence*, 473-475, 1983.

[SoB83] Solina, S. and Bajcsy, R., "Shape and function", in *Proc. SPIE Conference on Intelligent Robots and Computer Vision*, Vol. 726, 284–291, 1983.

[StB91a] Stark, L. and Bowyer, K., "Achieving generalized object recognition through reasoning about association of function to structure", *IEEE Transactions on Pattern Analysis and Machine Intelligence*, **13:**1097–1104, 1991.

[StB91b] Stark, L. and Bowyer, K., "Generic recognition through qualitative reasoning about 3-D shape and object function", in *Proc. IEEE Conference on Computer Vision and Pattern Recognition*, 251–256, 1991.

[StB92] Stark, L. and Bowyer, K., "Indexing function-based categories for generic recognition", in *Proc. IEEE Conference on Computer Vision and Pattern Recognition*, 795–797, 1992.

[SHGB93] Stark, L., Hoover, A., Goldgof, D., and Bowyer, K., "Function-based recognition from incomplete knowledge of shape", in *Proc. IEEE Workshop on Qualitative Vision*, 11–22, 1993.

[StF91] Strat, T. and Fischler, M., "Natural object recognition: A theoretical framework and its implementation", in *Proc. International Joint Conference on Artificial Intelligence*, 1991.

[StF95] Strat, T. and Fischler, M., "The role of context in computer vision", in *Proc. ICCV Workshop on Context-Based Vision*, 1995.

[SuP94] Sung, K. and Poggio, T., "Example-based learning for view-based human face detection", in *Proc. ARPA Image Understanding Workshop*, 747–756, 1994.

[WeK92] Weiss, S.M., and Kulikowski, C.A., *Computer Systems that Learn: Classification and Prediction Methods from Statistics, Neural Nets, Machine Learning and Expert Systems*, Morgan Kaufmann, San Mateo, CA, 1992.

[Win84] Winston, P.H., *Artificial Intelligence*, 2nd ed., Addison-Wesley, Reading, MA, 1984.

[WBKL83] Winston, P.H., Binford, T.O., Katz, B., and Lowry, M., "Learning physical descriptions from functional descriptions, examples, and precedents", in *Proc. National Conference on Artificial Intelligence*, 433–439, 1983.

[WKBM95] Wnek, J., Kaufman, K., Bloedorn, E., and Michalski, R.S., "Inductive learning system AQ15c: The method and user's guide", *Reports of the Machine Learning and Inference Laboratory*, MLI 95-4, George Mason University, Fairfax, VA, 1995.

[WCHBS95] Woods, K., Cook, D., Hall, L., Bowyer, K., and Stark, L, "Learning membership functions in a function-based object recognition system", *Journal of Artificial*

Intelligence Research, **3**:187–222, 1995.

[ZhB96] Zheng, Y. and Bhanu, B., "Performance improvement by input adaptation using modified Hebbian learning", in *Proc. ARPA Image Understanding Workshop*, 1381–1387, 1996.

[Zur92] Zurada, J.M., *Introduction to Artificial Neural Systems*, West Publishing, St. Paul, MN, 1992.